4896 *J. Chem. Eng. Data* **2010,** *55,* 4896–4902

Experimental Isobaric Vapor−Liquid Equilibrium for Binary Systems of Ethyl Methyl Carbonate + Methanol, + Ethanol, + Dimethyl Carbonate, or + Diethyl Carbonate at 101.3 kPa

Xuemei Zhang,[*,†] Jian Zuo,[†] and Chungui Jian[‡]

School of Chemical Engineering and Technology, Tianjin University, Tianjin, People's Republic of China, and Tianjin Univtech Co. Ltd., Tianjin, People's Republic of China

---

Isobaric vapor−liquid equilibrium (VLE) data were measured for the binary systems ethyl methyl carbonate (EMC) + methanol, + ethanol, + dimethyl carbonate (DMC), and + diethyl carbonate (DEC) at 101.3 kPa using a vapor−liquid equilibrium still. The thermodynamic consistency of the experimental data was verified by Herington[1] method. The experimental VLE data were correlated with the Wilson, NRTL, and UNIQUAC activity coefficient models. The results show that the calculated values of vapor phase mole fraction and boiling temperature by the Wilson, NRTL, and UNIQUAC models agree well with the experimental data. Futhermore, azeotropic behavior was observed for the binary system of ethanol + EMC.

Introduction

Ethyl methyl carbonate (EMC), an environmentally benign and asymmetric carbonic acid ester, is an excellent cosolvent for a nonaqueous electrolyte in the lithium battery for its such outstanding features as low viscosity, high dielectric constant, good solubility of lithium salts and high safety and stability. Compared with symmetric carbonates, such as dimethyl carbonate (DMC) and diethyl carbonate (DEC), EMC can improve the energy density, discharge capacity, safety, and life span of lithium batteries. Besides, EMC is an important carbonylation reagent, because it includes both methyl and ethyl groups and has the dual features of dimethyl carbonate and diethyl carbonate. It is also an excellent organic solvent with good compatibility with many organic solvents, such as alcohols, ketones, and esters. In view of this, many researchers devote themselves to developing synthesis methods for ethyl methyl carbonate. Among the various synthesis processes for ethyl methyl carbonate, the transesterification of DMC with ethanol is environmentally benign and has a relatively high reaction equilibrium constant and thus is considered as a feasible process.[2,3]

The reaction system contains the following five components: methanol, ethanol, DMC, EMC, and DEC, which implies a challenge in the separation. Although many contributions to the process parameters and the utilization of EMC have come forth,[4] those on the vapor−liquid equilibrium (VLE) data of EMC with other components are minimal. This situation has restricted the production of EMC to some extent, as vapor−liquid equilibrium data are generally the prerequisites for the design and analysis of separation processes of EMC from other components. Thus, in this work the VLE data have been measured and correlated by Wilson, NRTL, and UNIQUAC models, which provide the theoretical basis for design and analysis of the process of separation of EMC from other components.

Experimental Section

Materials. Methanol ($w = 0.999$) and ethanol ($w = 0.999$) were supplied by Tianjin Kewei Reagent Co. DMC ($w = 0.998$), EMC ($w = 0.999$), and DEC ($w = 0.999$) were provided by Hebei Chaoyang Chemical Co. All chemicals were AR grade materials. The GLC analysis failed to show any observable impurities for all the used chemicals. Physical properties, Antoine constants, and the measured vapors to literature correlations of the pure components are shown in Tables 1 to 3.

Table 1. Physical Properties of the Pure Components

component	methanol	ethanol	DMC	EMC	DEC
M/g·mol^{-1}	32.04[5]	46.07[5]	90.08[5]	104.10[7]	118.13[5]
T_b/K	337.8[5]	351.44[5]	363.7[5]	381.05[7]	400.0[5]
T_c/K	512.5[5]	514.0[5]	557.0[5]	560.75[7]	576.00[6]
p_c/MPa	8.084[5]	6.137[5]	4.80[5]	3.839[7]	3.39[6]
V_c/cm^3·mol^{-1}	117[5]	168[5]	252[5]	303.5[7]	346.0[6]
r	1.4311[6]	2.1055[6]	3.0613[6]	3.69[7]	3.7357[6]
q	1.432[6]	1.972[6]	2.816[6]	3.36[7]	3.356[6]

Table 2. Antoine Constants for the Pure Components

	Antoine constants[a]			
component	A	B	C	temperature range/K
methanol[7]	7.19736	1574.99	−34.29	175.47 to 512.5
ethanol[7]	7.33827	1650.50	−41.67	159.05 to 514.0
DMC[7]	6.4338	1413.00	−44.25	273.15 to 548.0
EMC[7]	6.4308	1466.437	−49.461	317.56 to 546.79
DEC[7]	5.883	1223.77	−84.304	230.15 to 576.0

[a] Antoine equation: $\log_{10}(P) = A - B/(T + C)$ with P/kPa and T/K.

Table 3. Measured Pure Component Vapor Pressures versus Literature Correlations

		p/kPa	
component	T/K	this work	literature correlation[7]
methanol	337.55	101.3	100.9
ethanol	351.45	101.3	102.4
DMC	363.45	101.3	101.6
EMC	381.25	101.3	102.6
DEC	399.65	101.3	100.5

Apparatus and Procedure. The VLE data at atmospheric pressure were measured using a circulation vapor−liquid equilibrium still (a modified Othmer still). The total volume of the still was about 60 cm^3 of which the liquid occupied about 50 cm^3. The details about this apparatus were described by Li et al.[8] During the experiments, the liquid was injected into the boiling chamber and heated. The vapor was condensed in the

---

[*] To whom correspondence should be addressed. Tel.: +86 02227409476. E-mail: zhangxuemei@tju.edu.cn.
[†] Tianjin University.
[‡] Tianjin Univtech Co. Ltd.

10.1021/je100494z

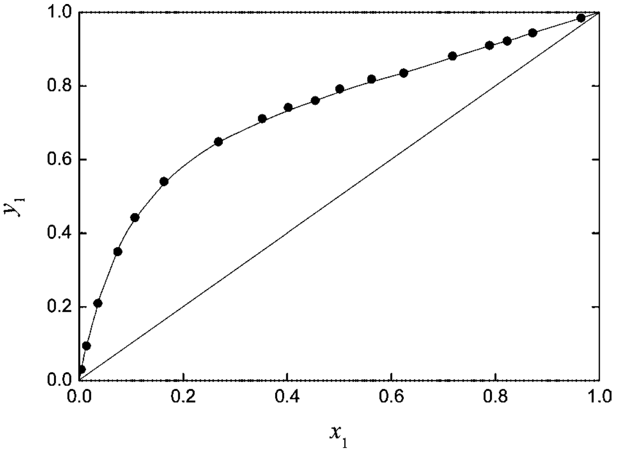

Figure 1. x_1, y_1 diagram for methanol (1) + water (2) system at 101.3 kPa. ●, this work; —, ref 6.

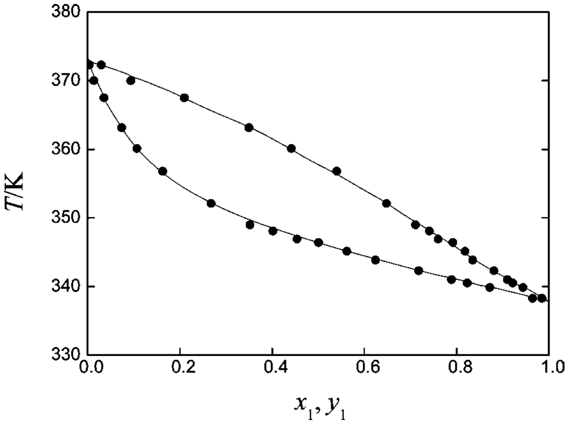

Figure 2. *T*, x_1, y_1 diagram for the methanol (1) + water (2) system at 101.3 kPa. ●, this work; —, ref 6.

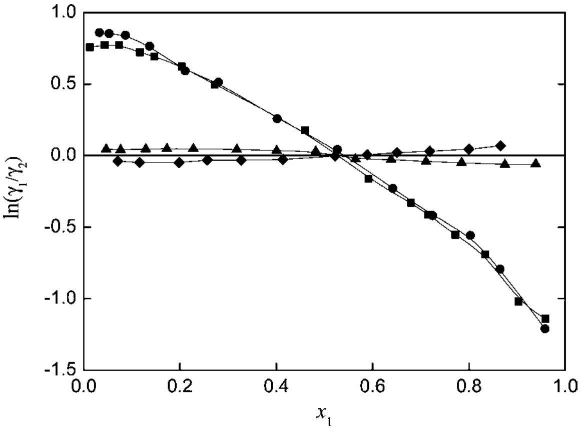

Figure 3. Thermodynamic consistency check. ■, methanol (1) + EMC (2); ●, ethanol + EMC (2); ▲, DMC (1) + EMC (2); ◆, EMC (1) + DEC (2).

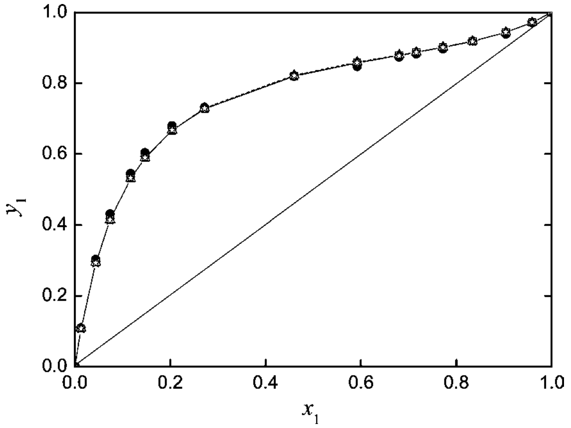

Figure 4. x_1, y_1 diagram for methanol (1) + EMC (2) system at 101.3 kPa. ●, experimental data in this work; □, correlated results by Wilson model; △, correlated results by NRTL model; ☆, correlated results by UNIQUAC model.

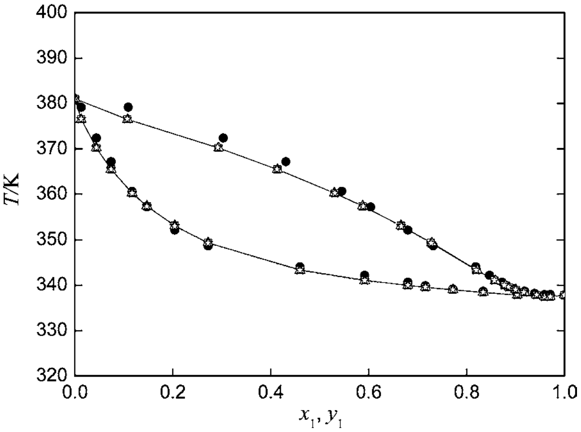

Figure 5. *T*, x_1, y_1 diagram for methanol (1) + EMC (2) system at 101.3 kPa. ●, experimental data in this work; □, correlated results by Wilson model; △, correlated results by NRTL model; ☆, correlated results by UNIQUAC model.

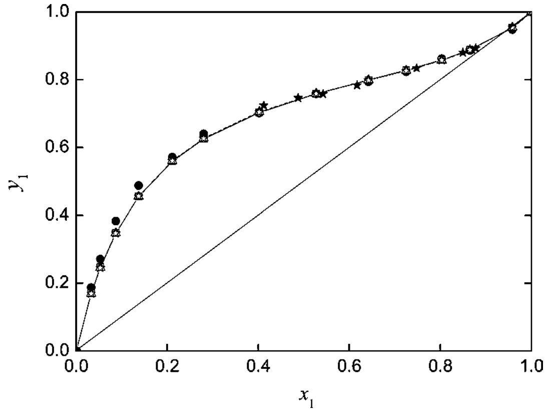

Figure 6. x_1, y_1 diagram for ethanol (1) + EMC (2) system at 101.3 kPa. ●, experimental data in this work; ★, literature data by Luo etal. (ref 12); □, correlated results by Wilson model; △, correlated results by NRTL model; ☆, correlated results by UNIQUAC model.

condenser and at the same time returned to the equilibrium chamber through the vapor phase sampling port. Both liquid and condensed vapor were continuously recirculated in the still to ensure that the liquid and vapor phases were in intimate contact during boiling. Equilibrium was assumed when constant vapor and liquid temperature was obtained in about (0.5 to 1) h. The system was maintained in the equilibrium state for about 30 min, and samples of the vapor and liquid phase were taken using a microsyringe from the sampling ports and then analyzed. This is done with minor disturbances on the equilibrium concentration and temperature since the size of the samples [(0.2 to 0.3) μL] is negligible compared to the volume of the still, 60 cm^3.

Temperatures were measured with Pt-100 probes connected to a digital temperature meter (AMETEK DTI-1000) with an uncertainty of ± 0.01 K according to the calibration certificate (ITS-90[9]). The pressure of the still was measured with a pressure transducer (Digiquartz 2300A) connected to a Digiquartz 740

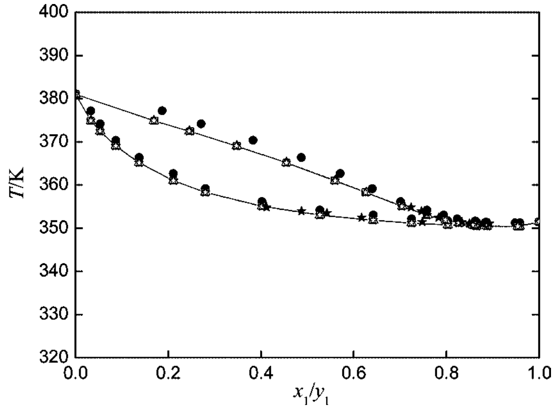

Figure 7. T, x_1, y_1 diagram for ethanol (1) + EMC (2) system at 101.3 kPa. ●, experimental data in this work; ★, literature data by Luo et al. (ref 12); □, correlated results by Wilson model; △, correlated results by NRTL model; ☆, correlated results by UNIQUAC model.

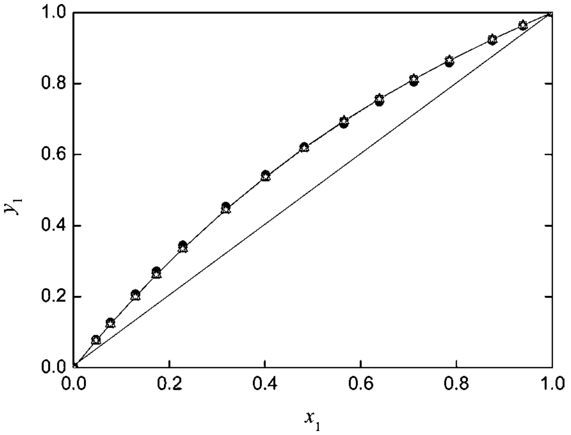

Figure 8. x_1, y_1 diagram for DMC (1) + EMC (2) system at 101.3 kPa. ●, experimental data in this work; □, correlated results by Wilson model; △, correlated results by NRTL model; ☆, correlated results by UNIQUAC model.

Table 4. Experimental VLE Data for the System of Methanol (1) + EMC (2) at 101.3 kPa

x_1	y_1	T/K	γ_1	γ_2
0.959	0.971	337.95	0.983	3.09
0.904	0.939	338.15	1.00	2.76
0.834	0.919	338.65	1.04	2.07
0.772	0.897	339.15	1.08	1.88
0.716	0.882	339.85	1.11	1.68
0.680	0.873	340.65	1.12	1.56
0.592	0.847	342.15	1.18	1.39
0.460	0.819	344.05	1.37	1.15
0.272	0.732	348.65	1.74	1.06
0.204	0.680	352.15	1.90	1.02
0.147	0.604	357.15	1.96	0.980
0.117	0.545	360.65	1.98	0.962
0.074	0.431	367.15	1.99	0.920
0.044	0.303	372.35	1.99	0.920
0.013	0.109	379.15	1.96	0.919

Table 5. Experimental VLE Data for the System of Ethanol (1) + EMC (2) at 101.3 kPa

x_1	y_1	T/K	γ_1	γ_2
0.958	0.948	351.25	0.965	3.24
0.865	0.886	351.35	0.995	2.20
0.803	0.862	351.65	1.03	1.80
0.725	0.823	352.15	1.07	1.63
0.642	0.794	353.05	1.12	1.41
0.527	0.758	354.15	1.25	1.20
0.402	0.701	356.15	1.41	1.09
0.280	0.640	359.15	1.64	0.983
0.211	0.571	362.65	1.71	0.947
0.137	0.487	366.35	1.96	0.913
0.087	0.383	370.35	2.11	0.910
0.053	0.271	374.15	2.15	0.917
0.033	0.187	377.15	2.15	0.911

Table 6. Experimental VLE Data for the System of DMC (1) + EMC (2) at 101.3 kPa

x_1	y_1	T/K	γ_1	γ_2
0.939	0.962	364.15	0.970	1.03
0.875	0.920	365.05	0.967	1.03
0.785	0.858	366.25	0.969	1.02
0.711	0.804	367.35	0.968	1.01
0.639	0.748	368.35	0.972	1.00
0.565	0.686	369.65	0.969	0.994
0.482	0.622	371.15	0.984	0.957
0.401	0.543	372.65	0.986	0.953
0.318	0.454	374.25	0.991	0.950
0.228	0.345	376.15	0.993	0.948
0.173	0.272	377.15	1.00	0.954
0.129	0.208	378.25	0.996	0.952
0.077	0.128	379.65	0.986	0.947
0.047	0.080	380.25	0.992	0.950

Table 7. Experimental VLE Data for the System of EMC (1) + DEC (2) at 101.3 kPa

x_1	y_1	T/K	γ_1	γ_2
0.866	0.924	383.25	0.958	0.896
0.800	0.880	384.50	0.952	0.911
0.719	0.822	385.65	0.956	0.929
0.651	0.769	386.95	0.950	0.932
0.589	0.716	388.15	0.944	0.938
0.522	0.655	389.25	0.944	0.948
0.414	0.545	391.15	0.937	0.964
0.327	0.450	392.65	0.938	0.970
0.257	0.368	394.15	0.936	0.966
0.198	0.290	395.15	0.930	0.977
0.116	0.178	396.95	0.927	0.974
0.071	0.113	397.95	0.935	0.972

Table 8. Thermodynamic Consistency Check Result for the Binary Systems EMC + Methanol, + Ethanol, + DMC, and + DEC at 101.3 kPa

system	D	J	$D - J$
methanol + EMC	2.72	19.21	$-16.45 < 10$
ethanol + EMC	2.07	12.63	$-10.56 < 10$
DMC + EMC	5.72	7.15	$-1.43 < 10$
EMC + DEC	6.25	7.46	$-1.21 < 10$

intelligent display unit (Paroscientific) with the accuracy in full scale 0.01 %. The range of the pressure measurement was from (0 to 2070) kPa with a temperature range from (219 to 390) K. The composition of the vapor and liquid samples was determined with a gas chromatograph SP-2100 supplied by Beijing Beifenruili Analysis Instrument Ltd. after calibration with gravimetrically prepared standard solutions. Thermal conductivity detector (TCD) was used together with a GDX-403 packed column (3 mm × 2 m). Hydrogen was used as the carrier gas. The column inlet pressure was 0.3 MPa. Detector and injector temperatures were kept at 423.15 K and 438.15 K respectively. The current for TCD was 170 mA. At least two analyses were made for each sample. The maximum uncertainty in mole fraction was ± 0.001.

Results and Discussion

VLE data of the binary system of methanol + water were measured at 101.3 kPa to check the apparatus and experimental procedure. The comparison of the experimental data with the literature data for x, y diagram and T, x, y diagram are shown in Figures 1 and 2, respectively. The absolute and relative errors in vapor phase mole fraction are 0.004 and 1.42 %, respectively. The absolute and relative errors in boiling temperature are 0.26

Table 9. Correlated Binary Interaction Parameters and Root-Mean-Square Deviations between Experimental and Calculated Values for the Binary Systems EMC + Methanol, + Ethanol, + DMC, and + DEC at 101.3 kPa

model	parameters	rmsd	
		$\sigma(y_1)$[a]	$\sigma(T)$[b]/K
	Methanol (1) + EMC (2)		
Wilson	$(\lambda_{12} - \lambda_{22})/R = 383.20$ K; $(\lambda_{21} - \lambda_{11})/R = 71.73$ K	0.009	1.11
NRTL ($\alpha = 0.30$)	$(g_{12} - g_{22})/R = 487.00$ K; $(g_{21} - g_{11})/R = -43.00$ K	0.010	1.14
UNIQUAC	$(u_{12} - u_{22})/R = -3.06$ K; $(u_{21} - u_{11})/R = 279.12$ K	0.009	1.11
	Ethanol (1) + EMC (2)		
Wilson	$(\lambda_{12} - \lambda_{22})/R = 260.82$ K; $(\lambda_{21} - \lambda_{11})/R = 193.71$ K	0.016	1.32
NRTL ($\alpha = 0.30$)	$(g_{12} - g_{22})/R = 465.01$ K; $(g_{21} - g_{11})/R = -28.86$ K	0.016	1.31
UNIQUAC	$(u_{12} - u_{22})/R = 33.55$ K; $(u_{21} - u_{11})/R = 139.25$ K	0.017	1.31
	DMC (1) + EMC (2)		
Wilson	$(\lambda_{12} - \lambda_{22})/R = -119.52$ K; $(\lambda_{21} - \lambda_{11})/R = 192.11$ K	0.007	1.06
NRTL ($\alpha = 0.30$)	$(g_{12} - g_{22})/R = 353.77$ K; $(g_{21} - g_{11})/R = -274.38$ K	0.007	1.05
UNIQUAC	$(u_{12} - u_{22})/R = 167.57$ K; $(u_{21} - u_{11})/R = -134.83$ K	0.007	1.06
	EMC (1) + DEC (2)		
Wilson	$(\lambda_{12} - \lambda_{22})/R = 1.39$ K; $(\lambda_{21} - \lambda_{11})/R = -51.83$ K	0.005	0.82
NRTL ($\alpha = 0.30$)	$(g_{12} - g_{22})/R = 237.79$ K; $(g_{21} - g_{11})/R = -246.44$ K	0.005	0.79
UNIQUAC	$(u_{12} - u_{22})/R = -221.84$ K; $(u_{21} - u_{11})/R = 288.82$ K	0.006	0.79

[a]

$$\sigma(y_1) = \sqrt{\sum_{i=1}^{n} \frac{(y_i^{\mathrm{cal}} - y_i^{\mathrm{exp}})^2}{n}}$$

[b]

$$\sigma(T) = \sqrt{\sum_{i=1}^{n} \frac{(T_i^{\mathrm{cal}} - T_i^{\mathrm{exp}})^2}{n}}$$

Table 10. Correlation Results for Methanol (1) + EMC (2) System at 101.3 kPa

	Wilson				NRTL				UNIQUAC			
x_1	y_1^{cal}	T^{cal}/K	γ_1^{cal}	γ_2^{cal}	y_1^{cal}	T^{cal}/K	γ_1^{cal}	γ_2^{cal}	y_1^{cal}	T^{cal}/K	γ_1^{cal}	γ_2^{cal}
0.959	0.971	337.41	1.00	3.17	0.971	337.42	1.00	3.15	0.971	337.42	1.00	3.15
0.904	0.943	337.81	1.02	2.60	0.943	337.82	1.02	2.60	0.943	337.83	1.02	2.61
0.834	0.918	338.40	1.05	2.12	0.918	338.41	1.05	2.12	0.917	338.42	1.05	2.14
0.772	0.901	338.98	1.09	1.83	0.901	338.98	1.09	1.83	0.900	339.00	1.09	1.84
0.716	0.887	339.55	1.13	1.64	0.887	339.52	1.13	1.63	0.886	339.55	1.13	1.65
0.680	0.878	339.95	1.16	1.54	0.879	339.91	1.16	1.53	0.877	339.94	1.16	1.55
0.592	0.857	341.07	1.24	1.36	0.859	340.99	1.25	1.34	0.857	341.03	1.25	1.36
0.460	0.819	343.38	1.40	1.18	0.822	343.28	1.41	1.17	0.820	343.29	1.41	1.18
0.272	0.727	349.34	1.69	1.05	0.729	349.35	1.69	1.05	0.728	349.25	1.70	1.05
0.204	0.666	353.02	1.80	1.03	0.666	353.09	1.80	1.02	0.667	352.98	1.81	1.03
0.147	0.588	357.30	1.90	1.01	0.588	357.38	1.90	1.01	0.589	357.30	1.90	1.01
0.117	0.531	360.18	1.96	1.01	0.530	360.25	1.95	1.01	0.531	360.20	1.95	1.01
0.074	0.414	365.42	2.02	1.00	0.414	365.45	2.02	1.00	0.413	365.48	2.02	1.00
0.044	0.293	370.18	2.06	1.00	0.294	370.16	2.07	1.00	0.292	370.23	2.05	1.00
0.013	0.107	376.50	2.10	1.00	0.108	376.46	2.12	1.00	0.107	376.52	2.08	1.00

Table 11. Correlation Results for Ethanol (1) + EMC (2) System at 101.3 kPa

	Wilson				NRTL				UNIQUAC			
x_1	y_1^{cal}	T^{cal}/K	γ_1^{cal}	γ_2^{cal}	y_1^{cal}	T^{cal}/K	γ_1^{cal}	γ_2^{cal}	y_1^{cal}	T^{cal}/K	γ_1^{cal}	γ_2^{cal}
0.958	0.953	350.38	1.00	3.04	0.954	350.41	1.00	2.98	0.954	350.41	1.00	2.97
0.865	0.888	350.44	1.03	2.24	0.887	350.48	1.03	2.25	0.887	350.49	1.03	2.25
0.803	0.858	350.69	1.07	1.92	0.857	350.73	1.06	1.93	0.857	350.74	1.06	1.94
0.725	0.828	351.15	1.12	1.64	0.827	351.18	1.12	1.64	0.826	351.19	1.11	1.65
0.642	0.799	351.8	1.19	1.43	0.799	351.81	1.19	1.43	0.798	351.81	1.19	1.44
0.527	0.758	353.04	1.31	1.25	0.759	353.01	1.31	1.25	0.758	353.01	1.31	1.25
0.402	0.703	355.09	1.47	1.13	0.705	355.04	1.48	1.12	0.704	355.03	1.47	1.13
0.280	0.625	358.30	1.66	1.06	0.627	358.28	1.66	1.05	0.626	358.24	1.66	1.05
0.211	0.559	361.01	1.78	1.03	0.560	361.02	1.78	1.03	0.560	360.98	1.78	1.03
0.137	0.455	365.12	1.92	1.01	0.455	365.16	1.91	1.01	0.455	365.14	1.91	1.01
0.087	0.348	369.00	2.01	1.00	0.348	369.04	2.00	1.00	0.347	369.04	2.00	1.00
0.053	0.247	372.41	2.07	1.00	0.246	372.44	2.07	1.00	0.245	372.46	2.06	1.00
0.033	0.170	374.83	2.11	1.00	0.169	374.85	2.10	1.00	0.169	374.87	2.09	1.00

Table 12. Correlation Results for DMC (1) + EMC (2) System at 101.3 kPa

	Wilson				NRTL				UNIQUAC			
x_1	y_1^{cal}	T^{cal}/K	γ_1^{cal}	γ_2^{cal}	y_1^{cal}	T^{cal}/K	γ_1^{cal}	γ_2^{cal}	y_1^{cal}	T^{cal}/K	γ_1^{cal}	γ_2^{cal}
0.939	0.964	363..23	1.00	1.01	0.964	363..23	1.00	1.01	0.964	363.23	1.00	1.01
0.875	0.924	364.11	1.00	1.00	0.924	364.10	1.00	1.01	0.924	364.11	1.00	1.00
0.785	0.865	365.40	1.00	0.997	0.865	365.39	1.00	0.997	0.865	365.41	1.00	0.996
0.711	0.812	366.51	1.00	0.995	0.812	366.50	1.00	0.994	0.812	366.52	1.00	0.994
0.639	0.756	367.65	1.00	0.994	0.757	367.63	1.01	0.992	0.756	367.65	1.00	0.993
0.565	0.694	368.86	1.00	0.994	0.695	368.84	1.01	0.992	0.694	368.87	1.00	0.994
0.482	0.618	370.28	1.00	0.995	0.619	370.27	1.01	0.993	0.618	370.28	1.00	0.995
0.401	0.536	371.73	1.00	0.996	0.537	371.72	1.00	0.994	0.537	371.72	1.00	0.996
0.318	0.445	373.27	1.00	0.998	0.445	373.27	1.00	0.996	0.445	373.26	1.00	0.997
0.228	0.335	375.01	0.997	0.999	0.335	375.02	0.998	0.998	0.335	375.00	0.998	0.999
0.173	0.262	376.10	0.995	0.999	0.262	376.12	0.995	0.999	0.262	376.09	0.996	0.999
0.129	0.200	377.00	0.993	1.00	0.200	377.02	0.992	0.999	0.200	376.99	0.994	1.00
0.077	0.123	378.08	0.991	1.00	0.123	378.10	0.988	1.00	0.123	378.08	0.992	1.00
0.047	0.076	378.72	0.990	1.00	0.076	378.73	0.986	1.00	0.077	378.71	0.991	1.00

Table 13. Correlation Results for EMC (1) + DEC (2) System at 101.3 kPa

	Wilson				NRTL				UNIQUAC			
x_1	y_1^{cal}	T^{cal}/K	γ_1^{cal}	γ_2^{cal}	y_1^{cal}	T^{cal}/K	γ_1^{cal}	γ_2^{cal}	y_1^{cal}	T^{cal}/K	γ_1^{cal}	γ_2^{cal}
0.866	0.927	382.02	0.997	0.900	0.927	382.06	0.997	0.893	0.928	382.08	0.997	0.884
0.800	0.884	383.21	0.994	0.916	0.885	383.26	0.993	0.912	0.886	383.29	0.993	0.902
0.719	0.827	384.70	0.989	0.932	0.826	384.77	0.987	0.931	0.827	384.81	0.986	0.924
0.651	0.773	385.98	0.983	0.945	0.772	386.05	0.980	0.945	0.773	386.10	0.979	0.941
0.589	0.719	387.17	0.976	0.955	0.719	387.23	0.973	0.956	0.719	387.29	0.972	0.954
0.522	0.657	388.47	0.968	0.965	0.656	388.52	0.965	0.967	0.655	388.58	0.962	0.967
0.414	0.546	390.58	0.954	0.978	0.545	390.61	0.951	0.980	0.543	390.64	0.947	0.984
0.327	0.447	392.29	0.941	0.989	0.446	392.30	0.939	0.988	0.443	392.29	0.934	0.993
0.257	0.360	393.67	0.929	0.992	0.360	393.66	0.928	0.993	0.358	393.60	0.925	0.997
0.198	0.284	394.82	0.919	0.995	0.284	394.80	0.919	0.996	0.283	394.69	0.920	1.00
0.116	0.171	396.40	0.904	0.998	0.171	396.38	0.906	0.999	0.173	396.24	0.918	1.00
0.071	0.106	397.26	0.895	0.999	0.107	397.24	0.899	1.00	0.109	397.12	0.922	1.00

K and 0.073 %, respectively. The experimental data of this work agree well with the literature data. Thus, the apparatus and experimental method are reliable and credible. The VLE data of the binary systems EMC + methanol, + ethanol, + DMC, and + DEC were measured at 101.3 kPa. The VLE data measured with the calculated activity coefficients are reported in Tables 4 to 7.

The general equilibrium relationship for VLE can be expressed as[10]

$$p\hat{\phi}_i^{V} y_i = p_i^{s}\phi_i^{s}\gamma_i x_i \exp\left(\frac{V_i^{L}(p - p_i^{s})}{RT}\right) \qquad (1)$$

where p and T are the total pressure and the temperature in the equilibrium system, respectively; x_i is the mole fraction of component i in liquid phase; y_i is the mole fraction of component i in vapor phase; γ_i is the activity coefficient of component i in the liquid phase; p_i^s is the saturation vapor pressure of pure liquid i at system temperature T, which can be obtained from the Antoine equation. ϕ_i^s is the fugacity coefficient of pure vapor i at equilibrium system temperature T and saturation vapor pressure p_i^s. $\hat{\phi}_i^V$ is the fugacity coefficient of component i in the vapor phase; V_i^L is the mole volume of pure liquid i.

The Poynting factor, the exponential term in eq 1, is close to unity at low or moderate pressure; eq 1 can be simplified to

$$p\hat{\phi}_i^{V} y_i = p_i^{s}\phi_i^{s}\gamma_i x_i \qquad (2)$$

The fugacity coefficients, ϕ_i^s and $\hat{\phi}_i^V$, were calculated by using the Soave−Redlich−Kwong (SRK) equation. The activity coefficient of component i in the liquid phase, γ_i, can be determined by eq 2. And the activity coefficients should satisfy the Gibbs−Duhem equation.[10] But experimental errors may cause deviation of the activity coefficients drawn from the experimental VLE data from the Gibbs−Duhem equation. Therefore, the thermodynamic consistency must be checked to

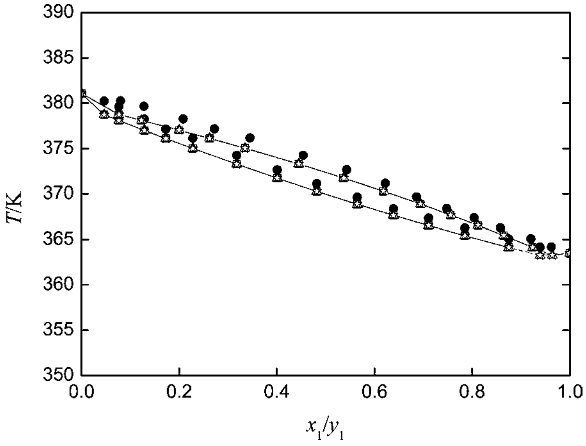

Figure 9. T, x_1, y_1 diagram for DMC (1) + EMC (2) system at 101.3 kPa. ●, experimental data in this work; □, correlated results by Wilson model; △, correlated results by NRTL model; ☆, correlated results by UNIQUAC model.

confirm whether the experimental VLE data are consistent with the Gibbs−Duhem equation. In this work, the thermodynamic consistency was checked by Herington method,[1] which can be expressed as follows

$$\int_{x_1=0}^{x_1=1} \ln \frac{\gamma_1}{\gamma_2} \, \mathrm{d}x_1 = 0 \tag{3}$$

$$D = 100 \cdot \left| \frac{S_+ - S_-}{S_+ + S_-} \right| = 100 \cdot \frac{\int_{x_1=0}^{x_1=1} \ln \frac{\gamma_1}{\gamma_2} \, \mathrm{d}x_1}{\int_{x_1=0}^{x_1=1} \ln \left| \frac{\gamma_1}{\gamma_2} \right| \mathrm{d}x_1} \tag{4}$$

$$J = 150 \cdot \frac{T\mathrm{max} - T\mathrm{min}}{T\mathrm{min}} \tag{5}$$

where S_+ and S_- are the area of region above the horizontal coordinate axis and that under the horizontal coordinate axis, respectively, as shown in Figure 3. $T_{\max}$ and $T_{\min}$ are the maximum and minimum boiling temperature in the studied systems, respectively.

Equation 3 does not usually equal zero exactly because of experimental errors, thus Herington presented a semiempirical method, in which the value of $D - J$ must be less than 10 for isobaric VLE. The test results of thermodynamic consistency are demonstrated in Figure 3. The values of D, J, and $D - J$ are shown in Table 8. The results show that the experimental VLE data for the binary systems EMC + methanol, + ethanol, + DMC, and + DEC at 101.3 kPa are thermodynamically consistent.

The experimental data were correlated using Wilson, NRTL, and UNIQUAC models.[10] The binary interaction parameters of all models are obtained minimizing the objective function F[11]

$$F = \sum_{k=1}^{\mathrm{NP}} \sum_{i}^{2} \left(\frac{\gamma_{i,k}^{\mathrm{exp}} - \gamma_{i,k}^{\mathrm{cal}}}{\gamma_{i,k}^{\mathrm{exp}}} \right)^2 \tag{6}$$

where NP is the number of experimental data and the superscripts “cal” and “exp” indicate the calculated and experimental values respectively. $\gamma_{i,k}^{\mathrm{exp}}$ is determined by eq 2 and $\gamma_{i,k}^{\mathrm{cal}}$ is calculated by the Wilson, NRTL, and UNIQUAC models.

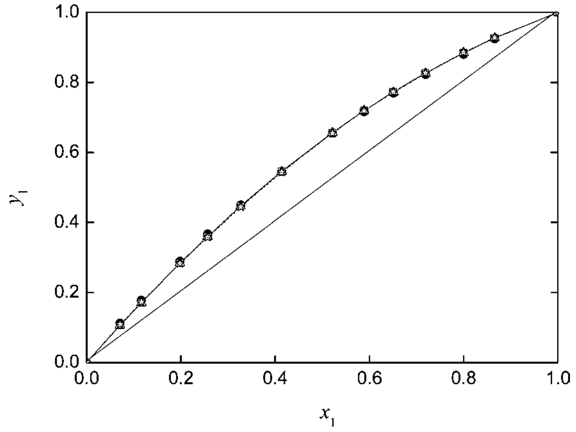

Figure 10. x_1, y_1 diagram for EMC (1) + DEC (2) system at 101.3 kPa. ●, experimental data in this work; □, correlated results by Wilson model; △, correlated results by NRTL model; ☆, correlated results by UNIQUAC model.

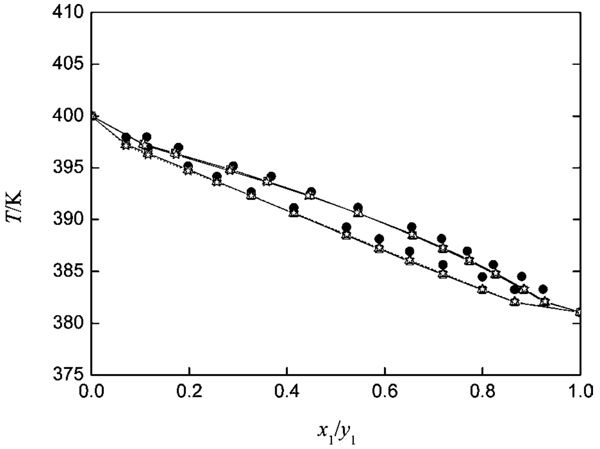

Figure 11. T, x_1, y_1 diagram for EMC (1) + DEC (2) system at 101.3 kPa. ●, experimental data in this work; □, correlated results by Wilson model; △, correlated results by NRTL model; ☆, correlated results by UNIQUAC model.

The correlated binary interaction parameters of the Wilson, NRTL, and UNIQUAC models for the binary systems EMC + methanol, + ethanol, + DMC, and + DEC at 101.3 kPa are shown in Table 9 together with the root-mean-square deviations (rmsd) of vapor mole fraction and bubble-point temperature. Vapor mole fraction, bubble-point temperature, and the liquid phase activity coefficients calculated using the correlated binary interaction parameters are given in Tables 10 to 13 and Figures 4 to 11.

It can be seen from Tables 10 to 13 and Figures 4 to 11 that the differences among the vapor phase mole fraction and boiling temperature calculated by the Wilson, NRTL, and UNIQUAC modes are indistinct. The RMSDs of the of vapor mole fraction and bubble-point temperature calculated by using the correlated parameters are not more than 0.017 and 1.32 K, respectively. Thus, all of the three models can predict the VLE data for the binary systems EMC + methanol, + ethanol, + DMC, and + DEC at 101.3 kPa well. It can also be seen from Figures 6 and 7 that azeotropic behavior exists in the ethanol−EMC system.

Conclusions

The isobaric VLE data of the binary systems EMC + methanol, + ethanol, + DMC, and + DEC at 101.3 kPa were measured using a vapor−liquid equilibrium still. The thermodynamic consistency test shows that the experimental VLE data are thermodynamically consistent. The Wilson, NRTL and UNIQUAC models are used to correlate the experimental data. The results show that the calculated values by the Wilson, NRTL, and UNIQUAC models agree well with the experimental data. Furthermore, there is azeotropic behavior in the ethanol−EMC system.

Literature Cited

(1) Ziqiang, Z.; Shanjing, Y.; Zhangli, J. *Principle and Application of Fluid Phase Equilibrium*; Zhejiang University Press: Hangzhou, 1990.
(2) Hong, G.; Marcus, J. P.; Esther, S. T. Method of synthesizing unsymmetric organic carbonates and preparing nonaqueous electrolytes for alkali ion electro- chemical cells U.S. Patent 5,962,720, 1999.
(3) Hiromi, O.; Hizuru, K.; Akiyoshi M. Nonaqueous secondary electrochemical battery U.S. Patent 5,525,443, 1996.
(4) Xu, L. Choosing and Controlling the Technical Process of Synthesizing Ethyl Methyl Carbonate by Exchanging of Ester. *Anhui Chem. Eng. (China)* **2006**, *142*, 35–37.
(5) David, R. L. *CRC Handbook of Chemistry and Physics*, 87th ed.; Taylor and Francis: Boca Raton, FL, 2007.
(6) Gmehling, J.; Onken, U.; Rearey-Nies, J. R. *Vapor-Liquid Equilibrium Data Collection*; DECHEMA: Frankfurt, 1988.
(7) Jiaquan, Y. *Chemical and phase equilibria of dimethyl carbonate, ethanol, ethyl methyl carbonate, enthanol, and diethyl carbonate mixture.* Master thesis, Department of Chemical and material Engineering, National Central University, Taiwan, 2008.
(8) Li, Q.; Xing, F.; Lei, Z.; Wang, B.; Chang, Q. Isobaric Vapor-Liquid Equilibrium for Isopropanol + Water + 1-Ethyl-3-methylimidazolium Tetrafluoroborate. *J. Chem. Eng. Data* **2008**, *53*, 275–279.
(9) Mangum, B. W.; Furukawa, G. T. *Guidelines for realizing the International Temperature Scale of 1990 (ITS-90)*; U.S. Department of Commerce, National Institute of Standards and Technology: Springfield, 1990.
(10) Smith, J. M.; Van, N. H. C.; Abbott, M. M. *Introduction to Chemical Engineering Thermodynamics*, 6th ed.; McGraw-Hill: New York, 2001.
(11) Guanghua, G.; Yangxin, Y. *Chemical Engineering Thermodynamics*; Tsinghua University Press: Beijing, 2000.
(12) Luo, H. P.; Xiao, W. D.; Zhu, K. H. Isobaric vapor−liquid equilibria of alkyl carbonates with alcohols. *Fluid Phase Equilib.* **2000**, *175*, 91–105.

Received for review May 11, 2010. Accepted August 24, 2010.

JE100494Z